A new subgrid characteristic length for turbulence simulations on anisotropic grids

F. X. Trias, A. Gorobets, M. H. Silvis, R. W. C. P. Verstappen, and A. Oliva

Citation: Physics of Fluids **29**, 115109 (2017);
View online: https://doi.org/10.1063/1.5012546
View Table of Contents: http://aip.scitation.org/toc/phf/29/11
Published by the American Institute of Physics

A new subgrid characteristic length for turbulence simulations on anisotropic grids

F. X. Trias,[1,a)] A. Gorobets,[1,2,b)] M. H. Silvis,[3,c)] R. W. C. P. Verstappen,[3,d)] and A. Oliva[1,e)]
[1]*Heat and Mass Transfer Technological Center, Technical University of Catalonia, C/Colom 11, 08222 Terrassa, Spain*
[2]*Keldysh Institute of Applied Mathematics, 4A, Miusskaya Sq., Moscow 125047, Russia*
[3]*Johann Bernoulli Institute for Mathematics and Computer Science, University of Groningen, P.O. Box 407, 9700 AK Groningen, The Netherlands*

(Received 12 May 2017; accepted 6 November 2017; published online 29 November 2017)

Direct numerical simulations of the incompressible Navier-Stokes equations are not feasible yet for most practical turbulent flows. Therefore, dynamically less complex mathematical formulations are necessary for coarse-grained simulations. In this regard, eddy-viscosity models for Large-Eddy Simulation (LES) are probably the most popular example thereof. This type of models requires the calculation of a subgrid characteristic length which is usually associated with the local grid size. For isotropic grids, this is equal to the mesh step. However, for anisotropic or unstructured grids, such as the pancake-like meshes that are often used to resolve near-wall turbulence or shear layers, a consensus on defining the subgrid characteristic length has not been reached yet despite the fact that it can strongly affect the performance of LES models. In this context, a new definition of the subgrid characteristic length is presented in this work. This flow-dependent length scale is based on the turbulent, or subgrid stress, tensor and its representations on different grids. The simplicity and mathematical properties suggest that it can be a robust definition that minimizes the effects of mesh anisotropies on simulation results. The performance of the proposed subgrid characteristic length is successfully tested for decaying isotropic turbulence and a turbulent channel flow using artificially refined grids. Finally, a simple extension of the method for unstructured meshes is proposed and tested for a turbulent flow around a square cylinder. Comparisons with existing subgrid characteristic length scales show that the proposed definition is much more robust with respect to mesh anisotropies and has a great potential to be used in complex geometries where highly skewed (unstructured) meshes are present. *Published by AIP Publishing.* https://doi.org/10.1063/1.5012546

I. INTRODUCTION

The Navier-Stokes (NS) equations are an excellent mathematical model for turbulent flows. However, direct numerical simulations are not feasible yet for most practical turbulent flows because the nonlinear convective term produces far too many scales of motion. Hence, in the foreseeable future, numerical simulations of turbulent flows will have to resort to models of the small scales. The most popular example thereof is Large-Eddy Simulation (LES). Briefly, the LES equations arise from applying a spatial filter, with filter length Δ, to the NS equations, resulting in

$$\partial_t \overline{\boldsymbol{u}} + (\overline{\boldsymbol{u}} \cdot \nabla)\overline{\boldsymbol{u}} = \nu \nabla^2 \overline{\boldsymbol{u}} - \nabla \overline{p} - \nabla \cdot \tau, \quad \nabla \cdot \overline{\boldsymbol{u}} = 0. \tag{1}$$

Here, $\overline{\boldsymbol{u}}$ is the filtered velocity and $\tau = \overline{\boldsymbol{u} \otimes \boldsymbol{u}} - \overline{\boldsymbol{u}} \otimes \overline{\boldsymbol{u}}$ is the subgrid stress (SGS) tensor that represents the effect of the unresolved scales. It is assumed that the filter $\boldsymbol{u} \to \overline{\boldsymbol{u}}$ commutes with differentiation. Since the SGS tensor, τ, depends not only on the filtered velocity, $\overline{\boldsymbol{u}}$, but also on the full velocity field, $\boldsymbol{u}$, we encounter a closure problem. We thus have to approximate τ by a tensor depending only on the filtered velocity, i.e., $\tau \approx \tau(\overline{\boldsymbol{u}})$.

Because of its inherent simplicity and robustness, the eddy-viscosity assumption is by far the most used closure model,

$$\tau(\overline{\boldsymbol{u}}) \approx -2\nu_e \mathsf{S}(\overline{\boldsymbol{u}}), \tag{2}$$

where ν_e denotes the eddy-viscosity and $\mathsf{S}(\overline{\boldsymbol{u}}) = 1/2(\nabla \overline{\boldsymbol{u}} + \nabla \overline{\boldsymbol{u}}^T)$ is the rate-of-strain tensor. Notice that $\tau(\overline{\boldsymbol{u}})$ is considered traceless without loss of generality because the trace can be included as part of the filtered pressure, $\overline{p}$. Then, most of the existing eddy-viscosity models can be expressed as follows:

$$\nu_e = (C_m \Delta)^2 D_m(\overline{\boldsymbol{u}}), \tag{3}$$

where C_m is the model constant, Δ is the subgrid characteristic length, and $D_m(\overline{\boldsymbol{u}})$ is the differential operator with units of frequency associated with the model. Here, no summation over m is implied.

In the last few decades research has primarily focused on either the calculation of the model constant, C_m, or the development of more appropriate model operators, $D_m(\overline{\boldsymbol{u}})$. An example of the former is the approach proposed by Lilly[1] to determine the model constant of the Smagorinsky model.[2]

a)xavi@cttc.upc.edu
b)andrey@cttc.upc.edu
c)m.h.silvis@rug.nl
d)r.w.c.p.verstappen@rug.nl
e)oliva@cttc.upc.edu

For an isotropic mesh, i.e., $\Delta = \Delta x = \Delta y = \Delta z$, and under the assumption that the cutoff wave number $k_c = \pi/\Delta$ lies within the inertial range of a universal Kolmogorov spectrum, $E(k) = C_K \varepsilon^{2/3} k^{-5/3}$, a model's constant, C_m, can be found by assuming that its dissipation is equal to the turbulent kinetic energy dissipation, ε. In this way, Lilly[1] obtained the Smagorinsky constant $C_S = (2/3C_K)^{3/4}/\pi$ (taking a value of $C_K \approx 1.58$ for the Kolmogorov constant[3] leads to $C_S \approx 0.17$).

The classical Smagorinsky model[2] has the disadvantage that its differential operator, $D_m(\overline{\boldsymbol{u}}) = |\mathsf{S}(\overline{\boldsymbol{u}})|$, does not vanish near solid walls. Early attempts to overcome this inherent problem of the Smagorinsky model made use of wall functions.[4,5] Later, Germano *et al.*[6] proposed the dynamic procedure, in which the constant C_m is computed with the help of the Jacobi identity (in least-squares sense), as was originally proposed by Lilly.[7] However, this approach leads to highly variable coefficient fields with a significant fraction of negative values for ν_e. This can cause numerical instability in simulations. Thus, averaging with respect to the homogeneous direction(s) and *ad hoc* clipping of ν_e are, in general, necessary. Therefore, the original dynamic procedure cannot be applied to geometrically complex flows without homogeneous directions. Several attempts to overcome these intrinsic limitations can be found in the literature: namely, the dynamic localization model and the Lagrangian dynamic model were, respectively, proposed by Ghosal *et al.*[8] and Meneveau *et al.*[9] In the same vein, Park *et al.*[10] introduced two global dynamic approaches: a dynamic global model based on the Germano identity[11] and a dynamic global model with two test filters based on the "global equilibrium" between the viscous dissipation and the SGS dissipation. Later, You and Moin[12] presented a dynamic global approach using only one test filter. Tejada-Martínez and Jansen[13,14] proposed an approach where the filter width ratio, the sole model parameter in a dynamic Smagorinsky model, is computed dynamically too. To do so, they assumed scale invariance and made use of a secondary test filter.

To construct models that vanish near solid walls, one can alternatively change the differential operator, $D_m(\overline{\boldsymbol{u}})$. Examples thereof are the WALE model,[15] Vreman's model,[16] the QR model,[17] and the σ-model.[18] This list can be completed with a novel eddy-viscosity model proposed by Ryu and Iaccarino[19] and two eddy-viscosity models recently proposed by the authors of this paper: namely, the S3PQR model[20] and the vortex-stretching-based eddy-viscosity model.[21]

Surprisingly, in the LES community, little attention has been paid to the computation of the subgrid characteristic length, Δ, which is also a key element of any eddy-viscosity model [see Eq. (3)]. Due to its simplicity and applicability to unstructured meshes, nowadays the most widely used approach to compute the subgrid characteristic length is the one proposed by Deardorff,[22] i.e., the cube root of the cell volume. For a Cartesian grid, it reads

$$\Delta_{\text{vol}} = (\Delta x \Delta y \Delta z)^{1/3}. \tag{4}$$

Extensions of this approach for anisotropic grids were proposed by Schumann,[23] Lilly,[24] and Scotti *et al.*[25] It was found that for small anisotropies, Deardorff's length scale is reasonably accurate, whereas corrections are required for highly anisotropic meshes, such as the pancake-like meshes that are often used to resolve near-wall turbulence or shear layers. For instance, the following correction was proposed by Scotti *et al.*:[25]

$$\Delta_{\text{Sco}} = f(a_1, a_2)\Delta_{\text{vol}}, \tag{5}$$

where $f(a_1, a_2) = \cosh\sqrt{4/27[(\ln a_1)^2 - \ln a_1 \ln a_2 + (\ln a_2)^2]}$ and $a_1 = \Delta x/\Delta z$ and $a_2 = \Delta y/\Delta z$, assuming that $\Delta x \le \Delta z$ and $\Delta y \le \Delta z$. Nevertheless, it is "*still assumed, however, that the small scale limit of the simulation is in the Kolmogorov inertial sub-range in all directions. This is a serious limitation as the most common reason for applying anisotropic resolution is an expectation of anisotropic and/or inhomogeneous turbulence, typically in regions close to a boundary.*"[24] The definition of Δ given in Eq. (5) was tested by Scotti *et al.*[26] for forced isotropic turbulence using highly anisotropic grids. They compared the correction factor $f(a_1, a_2)$ with the correction $f_{dyn}(a_1, a_2)$ obtained by applying the above-mentioned dynamic approach[6] to $C_m \Delta_{\text{vol}} f_{dyn}(a_1, a_2)$ (the dynamic approach is usually applied to find the model constant, C_m). They reached the conclusion that the dynamic model reproduces the correct trend for pancake-like grids ($a_2 = 1$, $\Delta x \ll \Delta y = \Delta z$) but fails for pencil-like ones ($a_1 = a_2$, $\Delta x = \Delta y \ll \Delta z$). Another limitation of the approach proposed by Scotti *et al.*[25] [see Eq. (5)] is that it is applicable only to structured Cartesian grids. To circumvent this, Colosqui and Oberai[27] proposed an extension applicable to unstructured meshes. They assume that the second-order structure function satisfies Kolmogorov's hypotheses.

Alternative definitions of the subgrid characteristic length scale, Δ, include the maximum of the cell sizes,

$$\Delta_{\max} = \max(\Delta x, \Delta y, \Delta z), \tag{6}$$

the L^2-norm of the tensor $\boldsymbol{\Delta} \equiv \text{diag}(\Delta x, \Delta y, \Delta z)$ divided by $\sqrt{3}$,

$$\Delta_{\text{L2}} = \sqrt{(\Delta x^2 + \Delta y^2 + \Delta z^2)/3}, \tag{7}$$

and the square root of the harmonic mean of the squares of the grid sizes

$$\Delta_{\text{Lapl}} = \sqrt{3/(1/\Delta x^2 + 1/\Delta y^2 + 1/\Delta z^2)}, \tag{8}$$

which is directly related to the largest eigenvalue of the discrete approximation of the (negative) Laplacian, $-\nabla^2$. The first definition, $\Delta_{\max}$, was originally proposed in the first presentation of the Detached-Eddy Simulation (DES) method by Spalart *et al.*[28] as a safer and robust definition of Δ.

More recent definitions of the subgrid characteristic length scale are also found in the context of DES. Namely, Chauvet *et al.*[29] introduced the concept of sensitizing Δ to the local velocity field. In particular, they made Δ dependent on the orientation of the vorticity vector, $\boldsymbol{\omega} = (\omega_x, \omega_y, \omega_z) = \nabla \times \boldsymbol{u}$,

$$\Delta_\omega = \sqrt{(\omega_x^2 \Delta y \Delta z + \omega_y^2 \Delta x \Delta z + \omega_z^2 \Delta x \Delta y)/|\boldsymbol{\omega}|^2}, \tag{9}$$

with some minor corrections to prevent indeterminate forms of type 0/0 (see the original paper[29] for details). The formulation was subsequently generalized for unstructured meshes

by Deck.[30] The definition of Δ_ω detects the alignment of the vorticity vector, $\boldsymbol{\omega}$, with an axis, e.g., if $\boldsymbol{\omega} = (0, 0, \omega_z)$, then Δ_ω reduces to $\sqrt{\Delta x \Delta y}$. This approach was motivated by the fact that $\Delta_{\max}$ results in an excessive generation of SGS dissipation in the initial region of shear layers typically resolved on highly anisotropic grids. In a DES, this results in an artificial delay of Kelvin-Helmholtz instabilities because the model switches from Reynolds-averaged Navier-Stokes (RANS) to LES mode further downstream. However, similar to Deardorff's definition of Δ given in Eq. (4), the definition given in Eq. (9) may still involve the smallest of the grid spacings. This may lead to very low values of eddy-viscosity.

To circumvent this problem, recently Mockett *et al.*[31] proposed the following flow-dependent subgrid characteristic length scale:

$$\tilde{\Delta}_\omega = \frac{1}{\sqrt{3}} \max_{n,m=1,\dots,8} |\boldsymbol{l}_n - \boldsymbol{l}_m|, \tag{10}$$

where $\boldsymbol{l} = \boldsymbol{\omega}/|\boldsymbol{\omega}| \times \boldsymbol{r}_n$ and $\boldsymbol{r}_n$ ($n = 1, \dots, 8$ for a hexahedral cell) are the locations of the cell vertices. The quantity $\tilde{\Delta}_\omega$ represents the diameter of the set of cross-product points, $\boldsymbol{l}_n$, divided by $\sqrt{3}$. In the above-described case with $\boldsymbol{\omega} = (0, 0, \omega_z)$, it reduces to $\tilde{\Delta}_\omega = \sqrt{(\Delta x^2 + \Delta y^2)/3}$. Therefore, it is $\mathcal{O}(\max\{\Delta x, \Delta y\})$ instead of $\Delta_{\max} = \Delta z$ (for the typical situation where $\Delta z > \Delta x$ and $\Delta z > \Delta y$) or $\Delta_\omega = \sqrt{\Delta x \Delta y}$. Thus "*unlike* Δ_ω, *definition* (10) *never leads to a strong effect of the smallest grid-spacing on the subgrid-scale* Δ *even though it achieves the desired decrease compared to the* $\Delta_{\max}$ *definition in the quasi-2D flow regions treated on strongly anisotropic grids.*"[32]

More recently, Shur *et al.*[32] proposed to modify the definition of $\tilde{\Delta}_\omega$ given in Eq. (10) by introducing a nondimensional function $0 \leq F_{KH}(VTM) \leq 1$, resulting in the Shear Layer Adapted (SLA) subgrid-scale

$$\Delta_{\text{SLA}} = \tilde{\Delta}_\omega F_{KH}(VTM), \tag{11}$$

where the Vortex Tilting Measure (VTM) is given by

$$VTM = \frac{|(\mathsf{S} \cdot \boldsymbol{\omega}) \times \boldsymbol{\omega}|}{\omega^2 \sqrt{-Q_{\tilde{\mathsf{S}}}}}, \tag{12}$$

where $\tilde{\mathsf{S}}$ is the traceless part of the rate-of-strain tensor, $\mathsf{S} = 1/2(\nabla\overline{\boldsymbol{u}} + \nabla\overline{\boldsymbol{u}}^T)$, i.e., $\tilde{\mathsf{S}} = \mathsf{S} - 1/3\text{tr}(\mathsf{S})\mathsf{I}$. Note that for incompressible flows $\text{tr}(\mathsf{S}) = \nabla \cdot \overline{\boldsymbol{u}} = 0$, therefore, $\tilde{\mathsf{S}} = \mathsf{S}$. Finally Q_{A} denotes the second invariant of a second-order tensor A, $Q_{\mathsf{A}} = 1/2\{\text{tr}^2(\mathsf{A}) - \text{tr}(\mathsf{A}^2)\}$. The vortex tilting measure is bounded, $0 \leq VTM \leq 1$, and it takes zero value when the vorticity is aligned with an eigenvector of S with eigenvalue λ_i, i.e., $\mathsf{S}\boldsymbol{\omega} = \lambda_i \boldsymbol{\omega}$. Therefore, the VTM can be viewed as a measure of how much the rate-of-strain tensor tilts the vorticity vector towards another direction. Finally, the function F_{KH} is aimed at unlocking the Kelvin-Helmholtz instability in the initial part of shear layers. Different functions F_{KH} were proposed by Shur *et al.*[32] with the basic requirements that $0 \leq F_{KH}(VTM) \leq 1$, $F_{KH}(0) = 0$, and $F_{KH}(1) = 1$.

Despite the above-mentioned length scales, so far no consensus has been reached on how to define the subgrid characteristic length scale, particularly when considering anisotropic or unstructured grids. In this work, we therefore propose a new flow-dependent subgrid characteristic length scale that is based on the subgrid stress tensor, τ, and its representations on different grids. This simple and robust definition of Δ reduces the effect of mesh anisotropies on the performance of SGS models.

The structure of this paper is as follows. In Sec. II, all the above-mentioned definitions of the subgrid characteristic length are compared and classified on the basis of a list of desirable properties. These properties are based on physical, numerical, and/or practical arguments. Then, within this framework, a new subgrid characteristic length, based on the Taylor-series expansion of the SGS tensor in the computational space, is proposed in Sec. III. Moreover, in Sec. IV, a simple extension of this length scale for unstructured grids is proposed. In Sec. V, the newly proposed length scale is tested in wall-resolved large-eddy simulations on highly anisotropic structured grids (test cases: decaying isotropic turbulence and a plane-channel flow) and unstructured grids (test case: turbulent flow around a square cylinder), confirming that it is a robust definition that reduces the effects of mesh anisotropies on the performance of LES models. Finally, relevant results are summarized and conclusions are given in Sec. VI.

II. PROPERTIES OF THE SUBGRID CHARACTERISTIC LENGTH

Starting from the classical Smagorinsky model,[2] many eddy-viscosity models [see Eq. (2)] have been proposed (see the work of Trias *et al.*[20] for a recent review). The definition of ν_e given in Eq. (3) provides a general template for most of them. Therefore, a subgrid characteristic length, Δ, which is commonly associated with the local grid size, is required. Hence, for isotropic grids, Δ is equal to the mesh size, i.e., $\Delta = \Delta x = \Delta y = \Delta z$. However, for anisotropic or unstructured grids, a consensus on defining the subgrid characteristic length has not been reached yet. Despite the fact that in some situations it may provide very inaccurate results, three and a half decades later, the approach proposed by Deardorff,[22] i.e., the cube root of the cell volume [see Eq. (4)], is by far the most widely used.

Alternative methods to compute the subgrid characteristic length scale, Δ, have been reviewed in Sec. I. They are classified in Table I according to a list of desirable properties for a (proper) definition of Δ. These properties are based on physical, numerical, and/or practical arguments. Namely, the first property, denoted as **P1**, entails both positiveness and locality. Although from a physical point of view negative values of ν_e may be justified with the backscatter phenomenon, from a numerical point of view, the condition $\nu_e \geq 0$ is, in general, considered appropriate because it guarantees stability. Further, the LES equations should be Galilean invariant. In order to preserve this physical principle, the flow-dependent definitions of Δ (see property **P3**) are based on invariants derived from the gradient of the resolved velocity field, $\mathsf{G} \equiv \nabla\overline{\boldsymbol{u}}$. In doing so, the condition of locality is also achieved. From a practical point of view, locality is a desirable feature especially if the model is aimed to be applied in complex flows. The second property (**P2**) requires that Δ is properly bounded, i.e., given a

TABLE I. Properties of different definitions of the subgrid characteristic length, Δ. Namely, **P1**: positive (Δ ≥ 0), local, and frame invariant; **P2**: bounded, i.e., given a structured Cartesian mesh where $\Delta x \le \Delta y \le \Delta z$, $\Delta x \le \Delta \le \Delta z$; **P3**: sensitive to the local flow field; **P4**: applicable to unstructured meshes; **P5**: computational cost.

Formula	Δ_{vol} Equation (4)	Δ_{Sco} Equation (5)	Δ_{max} Equation (6)	Δ_{L2} Equation (7)	Δ_{Lapl} Equation (8)	Δ_{ω} Equation (9)	$\tilde{\Delta}_{\omega}$ Equation (10)	Δ_{SLA} Equation (11)	Δ_{lsq} Equation (18)
P1	Yes	Yes	Yes	Yes	Yes	Yes	Yes	Yes	Yes
P2	Yes	Yes	Yes	Yes	Yes	Yes	Yes	Yes	Yes
P3	No	No	No	No	No	Yes	Yes	Yes	Yes
P4	Yes	No	No[a]	No	No[a]	No[b]	Yes	Yes	Yes
P5	Low	Medium	Low	Low	Low	Medium	High	High	Low

[a]Possible with some adaptations.
[b]Deck[30] proposed a generalization for unstructured meshes.

structured Cartesian mesh where $\Delta x \le \Delta y \le \Delta z$, we need $\Delta x \le \Delta \le \Delta z$. These first two properties **P1** and **P2** are achieved by all the length scales shown in Table I. The third property (**P3**) classifies the methods to compute Δ in two families: those that solely depend on geometrical properties of the mesh and those that are also dependent on the local flow topology, i.e., the velocity gradient, G.

Assuming that the grid is Cartesian, we can express the subgrid characteristic length scales that are fully mesh-based in terms of the properties of the following second-order diagonal tensor:

$$\Delta \equiv \mathrm{diag}(\Delta x, \Delta y, \Delta z). \tag{13}$$

We take $\Delta x \le \Delta y \le \Delta z$ without loss of generality. Indeed the aforementioned mesh-based length definitions can be written as

$$\Delta_{vol} = R_{\Delta}^{1/3}, \Delta_{Sco} = f(a_1, a_2) R_{\Delta}^{1/3}, \Delta_{max} = \lambda_1^{\Delta},$$
$$\Delta_{L2} = \sqrt{\frac{\mathrm{tr}(\Delta^2)}{3}} = \sqrt{\frac{P_{\Delta}^2 - 2Q_{\Delta}}{3}}, \tag{14}$$

where the correction function $f(a_1, a_2)$ was defined in Eq. (5), $a_1 = \Delta x/\Delta z$, and $a_2 = \Delta y/\Delta z$. Moreover, $P_{\Delta} = \mathrm{tr}(\Delta)$, $Q_{\Delta} = 1/2\{\mathrm{tr}^2(\Delta) - \mathrm{tr}(\Delta^2)\}$, and $R_{\Delta} = \det(\Delta) = 1/6\{\mathrm{tr}^3(\Delta) - 3\mathrm{tr}(\Delta)\mathrm{tr}(\Delta^2) + 2\mathrm{tr}(\Delta^3)\}$ represent the first, second, and third invariants of the second-order tensor Δ, respectively. The three eigenvalues, $\lambda_1^{\Delta} \ge \lambda_2^{\Delta} \ge \lambda_3^{\Delta}$, of Δ are solutions of the characteristic equation $\det(\lambda \mathsf{I} - \Delta) = \lambda^3 - P_{\Delta}\lambda^2 + Q_{\Delta}\lambda - R_{\Delta} = 0$.

The aforementioned characteristic length scale definitions that depend on both the mesh and the flow topology can also be expressed in terms of invariants, namely, the invariants of Δ, the velocity gradient G, and G's symmetric and antisymmetric parts. To this end, note that the vorticity vector $\boldsymbol{\omega} = (\omega_x, \omega_y, \omega_z) = \nabla \times \overline{\boldsymbol{u}}$ can be expressed in terms of the rate-of-rotation tensor $\Omega = 1/2(\mathsf{G} - \mathsf{G}^T)$ as $\omega_k = -\epsilon_{ijk}\Omega_{ij}$, where ϵ_{ijk} is the Levi-Civita symbol. Here, summation over repeated indices is implied. Finally, the symmetric part of G is the rate-of-strain tensor, $\mathsf{S} = 1/2(\mathsf{G} + \mathsf{G}^T)$. These are the flow-dependent quantities required to compute the definitions of Δ of Chauvet *et al.*[29] [see the definition of Δ_{ω} given in Eq. (9)] and Mockett *et al.*[31] [see the definition of $\tilde{\Delta}_{\omega}$ given in Eq. (10)] and the modification Δ_{SLA} proposed by Shur *et al.*[32] [see Eq. (11)].

The last two desirable properties of subgrid characteristic length scales are of practical interest. Namely, property **P4** refers to the applicability of the method for unstructured meshes. Among the definitions of Δ that do not depend on the local flow, only the approach of Deardorff[22] can be straightforwardly used for unstructured grids. Recent flow-dependent definitions of Δ are potentially applicable for unstructured grids, although some of them have a relatively high computational cost. In this regard, to complete the list of properties, it is also desirable that the definition of Δ is well conditioned and has a low (or moderate) computational cost (property **P5**). In this respect, flow-dependent definitions of Δ may be problematic, having a significantly higher computational cost. Moreover, they require special attention for indeterminate forms of type 0/0.

The new definition of the subgrid characteristic length, Δ_{lsq}, which is presented in Sec. III matches all the above-mentioned properties with an inherent simplicity and a moderate computational cost.

III. BUILDING A NEW SUBGRID CHARACTERISTIC LENGTH

Several approaches to compute the subgrid characteristic length, Δ, can be found in the literature (see Sec. I). Their properties have been analyzed and compared in Sec. II (see Table I). As remarked before, despite these existing length scales, no consensus has been reached on how to define the subgrid characteristic length scale, particularly for (highly) anisotropic or unstructured grids. In this section, we therefore propose a new flow-dependent subgrid characteristic length scale that is based on the subgrid stress tensor, τ, and its representations on different grids.

The subgrid characteristic length, Δ, appears in a natural way when we consider the lowest-order approximation of the subgrid stress tensor, $\tau = \overline{\boldsymbol{u} \otimes \boldsymbol{u}} - \overline{\boldsymbol{u}} \otimes \overline{\boldsymbol{u}}$, i.e., the unclosed term in the filtered Navier-Stokes equations, Eq. (1). The approximation of the subgrid stress is obtained by approximating the residual velocity $u' = u - \overline{u}$.

To start, we restrict ourselves to one spatial direction and consider a box filter. The residue of the box filter can be related to the error of the midpoint rule for numerical integration, denoted by ϵ here. We have $\overline{u} = \int_{x-\Delta x/2}^{x+\Delta x/2} u(x)\,dx = \Delta x u(x) + \epsilon$ with $\epsilon = \frac{\Delta x^3}{24}\partial_x\partial_x u(c)$, where c lies somewhere in between $x - \Delta x/2$ and $x + \Delta x/2$. An expression for the residue of the one-dimensional box filter is then obtained by dividing

this error by $-\Delta x$ and adding u. Thus to lowest order, we get $u'(x) = -\frac{\Delta x^2}{24}\partial_x\partial_x u(x) + \mathcal{O}(\Delta x^4)$.

On a three-dimensional, isotropic grid, i.e., $\Delta = \Delta x = \Delta y = \Delta z$, the above approximation of the residue becomes $u' = -\frac{\Delta^2}{24}\nabla\cdot\nabla u + \mathcal{O}(\Delta^4)$. With the help of this approximation, it can be shown that the subgrid stress tensor is given by[33]

$$\tau(\overline{\boldsymbol{u}}) = \frac{\Delta^2}{12}\mathsf{G}\mathsf{G}^T + \mathcal{O}(\Delta^4). \tag{15}$$

The leading-order term in Eq. (15) is the gradient model proposed by Clark *et al.*,[33] where Δ denotes the filter length. Equation (15) has been derived for the box filter. However, it can be shown that the same result is obtained for any convolution filter with a symmetric kernel.[34]

We stress that in the above derivation, the grid is assumed to be isotropic, that is, $\Delta = \Delta x = \Delta y = \Delta z$. For an anisotropic grid, we can postulate that the lowest-order approximation of the subgrid stress also provides us with $\tau(\overline{\boldsymbol{u}}) \approx \frac{\Delta^2}{12}\mathsf{G}\mathsf{G}^T$, that is, the approximation (1) depends quadratically on the velocity gradient, (2) is given by a symmetric tensor, (3) is invariant under a rotation of the coordinate system, and (4) is proportional to Δ^2. Here, however, we do not yet know how to define the filter length, Δ, because the grid is anisotropic. For the gradient model, however, we can define the filter length by mapping the anisotropic mesh onto an isotropic mesh. Therefore we consider the coordinate transformations $\hat{x} = x/\Delta x$, $\hat{y} = y/\Delta y$, and $\hat{z} = z/\Delta z$. Expanding the subgrid stress as before, but now in the new, isotropic, coordinate system $\hat{x}, \hat{y}, \hat{z}$, and applying the chain rule for differentiation we obtain

$$\tau(\overline{\boldsymbol{u}}) = \frac{1}{12}\mathsf{G}_\Delta\mathsf{G}_\Delta^T + \mathcal{O}(\Delta^4). \tag{16}$$

Here, the velocity gradient on the anisotropic grid is defined as

$$\mathsf{G}_\Delta \equiv \mathsf{G}\Delta, \tag{17}$$

where Δ is the second-order tensor containing the mesh information given by Eq. (13). Equation (16) does not require an explicit definition of the filter length Δ. In fact the filter length is hidden in G_Δ and is not represented by a scalar but by the tensor Δ. Since both Eqs. (15) and (16) represent the lowest-order approximation of the subgrid stress, we can equate them and thus define the filter length Δ in Eq. (15) for anisotropic meshes. Here it may be remarked that we equate tensors; hence, the equality is to be understood in least-square sense. This leads to the following flow-dependent definition of Δ:

$$\Delta_{\mathrm{lsq}} = \sqrt{\frac{\mathsf{G}_\Delta\mathsf{G}_\Delta^T : \mathsf{G}\mathsf{G}^T}{\mathsf{G}\mathsf{G}^T : \mathsf{G}\mathsf{G}^T}}. \tag{18}$$

We first remark that this length scale reduces to Δ on an isotropic mesh. Second, since Δ_{lsq} is formally based on the lowest-order approximation of the subgrid stress, we see it as a generic way to define the filter length. It can thus be applied in any turbulence model, not just in eddy-viscosity models, Eq. (3). With respect to the properties discussed in Sec. II, the characteristic length scale given by Eq. (18) depends on the velocity gradient G. Therefore, it is locally defined and is frame invariant (**P1**). Moreover, Δ_{lsq} is obviously sensitive to flow orientation (property **P3**).

Furthermore, it may be noted that the numerator in Eq. (18) can be viewed as the Frobenius norm of the tensor $\mathsf{G}^T\mathsf{G}\Delta$, i.e., $\mathsf{G}_\Delta\mathsf{G}_\Delta^T : \mathsf{G}\mathsf{G}^T = \mathrm{tr}(\mathsf{G}_\Delta\mathsf{G}_\Delta^T\mathsf{G}\mathsf{G}^T) = \mathrm{tr}(\mathsf{G}\Delta^2\mathsf{G}^T\mathsf{G}\mathsf{G}^T) = \mathrm{tr}(\Delta\mathsf{G}^T\mathsf{G}(\Delta\mathsf{G}^T\mathsf{G})^T) = \Delta\mathsf{G}^T\mathsf{G} : \Delta\mathsf{G}^T\mathsf{G}$. Moreover, $\mathsf{G}\mathsf{G}^T : \mathsf{G}\mathsf{G}^T = \mathrm{tr}(\mathsf{G}\mathsf{G}^T\mathsf{G}\mathsf{G}^T) = \mathrm{tr}(\mathsf{G}^T\mathsf{G}\mathsf{G}^T\mathsf{G}) = \mathsf{G}^T\mathsf{G} : \mathsf{G}^T\mathsf{G}$, so we can also express Δ_{lsq} as

$$\Delta_{\mathrm{lsq}} = \sqrt{\frac{\Delta\mathsf{G}^T\mathsf{G} : \Delta\mathsf{G}^T\mathsf{G}}{\mathsf{G}^T\mathsf{G} : \mathsf{G}^T\mathsf{G}}}. \tag{19}$$

From this definition, it is obvious that Δ_{lsq} is positive and well bounded (properties **P1** and **P2**). Its applicability for unstructured meshes (property **P4**) relies on the proper adaptation of the tensor Δ (see Sec. IV). Regarding property **P5**, the computational cost of Δ_{lsq} is relatively small when compared to the other flow-dependent (property **P3**) length scales discussed in this paper, and special attention is only required for indeterminate forms of type 0/0.

The inherent simplicity and mathematical properties of the proposed length scale, as well as its basis in representations of the subgrid stress tensor on different grids, suggest that it can be a robust definition that minimizes the effects of mesh anisotropies on the performance of LES models. Note that the definition of Δ_{lsq} provided in Eq. (18) was already presented and partially evaluated during the Stanford CTR Summer Program 2016[35] and the CEAA'16 conference.[36]

To get a better understanding of Δ_{lsq}, we consider several special cases. First of all, as remarked before, this length scale reduces to Δ on an isotropic mesh. Second, for purely rotating flows, i.e., $\mathsf{S} = 0$ and $\mathsf{G} = \Omega$, Δ_{lsq} reduces to

$$\Delta_{\mathrm{lsq}} = \sqrt{\frac{\omega_x^2(\Delta y^2 + \Delta z^2) + \omega_y^2(\Delta x^2 + \Delta z^2) + \omega_z^2(\Delta x^2 + \Delta y^2)}{2|\boldsymbol{\omega}|^2}}, \tag{20}$$

which resembles the definition of $\Delta_{\boldsymbol{\omega}}$ proposed by Chauvet *et al.*[29] given in Eq. (9). Actually, similar to the definition of Δ proposed by Mockett *et al.*[31] given in Eq. (10), Δ_{lsq} is $\mathcal{O}(\max\{\Delta x, \Delta y\})$ instead of $\Delta_{\boldsymbol{\omega}} = \sqrt{\Delta x\Delta y}$. Therefore, it also avoids a strong effect of the smallest grid-spacing. Finally, results obtained for a simple 2D mesh and flow,

$$\Delta = \begin{pmatrix} \beta & 0 \\ 0 & \beta^{-1} \end{pmatrix}, \quad \mathsf{G} = \begin{pmatrix} 0 & 1 \\ 1-2\omega & 0 \end{pmatrix}, \tag{21}$$

are displayed in Fig. 1. Notice that the size of the control volume remains equal to unity; therefore, $\Delta_{\mathrm{vol}} = 1$, regardless of the value of β. On the other hand, values of ω in Fig. 1 range from a pure shear flow ($\omega = 0$) to a simple shear flow ($\omega = 1/2$) and to a pure rotating flow ($\omega = 1$). For the two limiting situations, $\Delta_{\mathrm{lsq}} = \sqrt{(\beta^2 + \beta^{-2})/2}$, whereas for $\omega = 1/2$, it reads $\Delta_{\mathrm{lsq}} = \beta^{-1}$. Recalling that in the particular case $\Delta x = \beta$ and $\Delta y = \beta^{-1}$, $\Delta_{\mathrm{lsq}} = \sqrt{(\Delta x^2 + \Delta y^2)/2}$ for $\omega = 0$ (pure shear) and $\omega = 1$ (pure rotation), whereas $\Delta_{\mathrm{lsq}} = \Delta y$ for the simple shear flow with $\omega = 1/2$. The latter corresponds quite well with the typical quasi-2D grid-aligned flow in the initial region of a shear layer. As it could be expected, the computed Δ_{lsq} is equal to the grid size in the direction orthogonal to the shear layer. The pure rotating flow ($\omega = 1$) is just a particular case of Eq. (20) with $\omega_x = \omega_y = 0$ and $\omega_z = 1$.

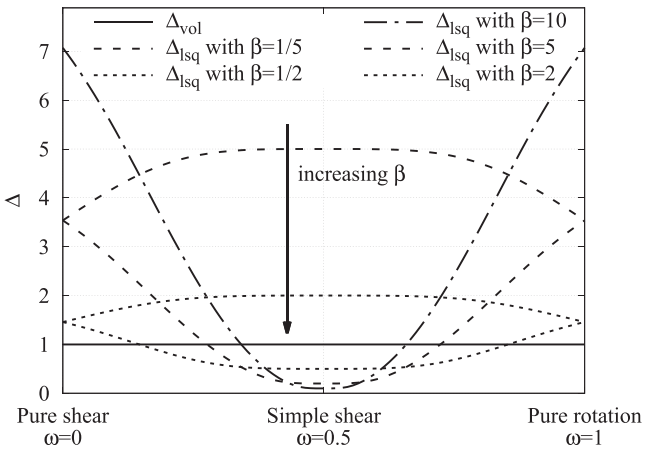

FIG. 1. Comparison between Δ_{lsq} and Δ_{vol} for the simple 2D flow defined in Eq. (21) with different values of $\beta = \{1/5, 1/2, 2, 5, 10\}$.

In order to study in more detail the effect of mesh anisotropies for different definitions of Δ, let us consider a Cartesian mesh with $\Delta x = \Delta y = 1$ and $\Delta z = \alpha$. In this case, the geometry-dependent definitions of Δ result in

$$\Delta_{\mathrm{vol}} = \alpha^{1/3}, \quad \Delta_{\mathrm{Sco}} = f(\min(\alpha, \alpha^{-1}), \min(1, \alpha^{-1})),$$
$$\Delta_{\mathrm{max}} = \max(1, \alpha), \quad \Delta_{\mathrm{L2}} = \sqrt{\frac{2+\alpha^2}{3}}, \quad \Delta_{\mathrm{Lapl}} = \sqrt{\frac{3\alpha^2}{2\alpha^2+1}}. \tag{22}$$

These functions are displayed in Fig. 2 using a log-log scale. Values of $\alpha > 1$ correspond to pencil-like meshes ($\Delta x = \Delta y \ll \Delta z$), whereas values of $\alpha < 1$ correspond to pancake-like meshes ($\Delta x \ll \Delta y = \Delta z$). Averaged results of Δ_{lsq} are also displayed; they have been obtained from a large sample of random traceless velocity gradient tensors, G. Notice that this simple random procedure was able to produce fairly good predictions to determine the model constant, C_m, for different SGS models.[20] Among all the geometry-dependent definitions, for the mesh considered here, the closest to $\langle \Delta_{\mathrm{lsq}} \rangle$ by far is the definition of Δ_{L2} given in Eq. (7). Actually, for very simple flow configurations such as pure shear or pure rotation, Δ_{lsq} reduces to Δ_{L2}. The second closest is the correction proposed by Scotti *et al.*[25] [see Eq. (5)]. Finally, Δ_{Lapl} is the only

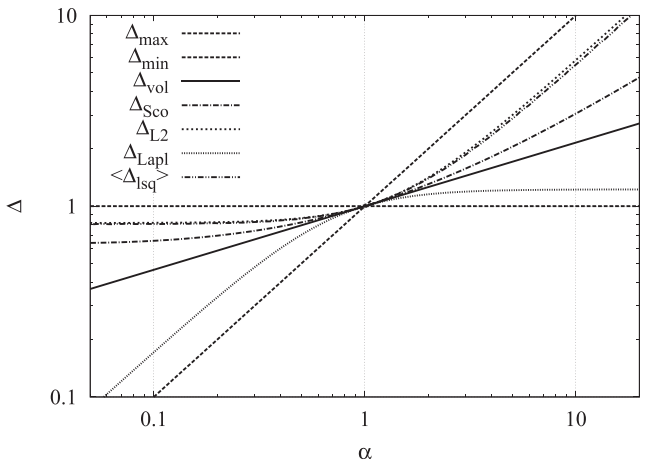

FIG. 2. Scaling of different definitions of Δ for a Cartesian mesh with $\Delta x = \Delta z = 1$ and $\Delta y = \alpha$. Average results of Δ_{lsq} have been obtained from a large sample of random traceless velocity gradient tensors.

definition that predicts values of Δ smaller than the classical Deardorff definition Δ_{vol}.

IV. JACOBIAN-BASED EXTENSION FOR UNSTRUCTURED MESHES

In Sec. III, a new method to compute the subgrid characteristic length has been proposed. Although it has been derived in the context of Cartesian meshes, the idea can be extended to unstructured meshes by noticing that it basically consists in projecting the leading term of the Taylor series expansion of τ [see Eq. (16)] onto the basic gradient model [see Eq. (15)].

For non-uniform Cartesian grids, we considered the coordinate transformations $\hat{x} = x/\Delta x$, $\hat{y} = y/\Delta y$, and $\hat{z} = z/\Delta z$. This led to a new, isotropic, coordinate system $\hat{x}, \hat{y}, \hat{z}$. Then, applying the chain rule for differentiation yielded the approximation of the subgrid stress tensor of Eq. (16). More generally, let $\xi_i(x_i)$ be a monotonic differentiable function that defines a mapping from the physical space in the i-direction, x_i, to the so-called computational space, ξ_i. Using the chain rule, we obtain

$$\frac{\partial \phi}{\partial x_i} = \frac{\partial \phi}{\partial \xi_i}\frac{d\xi_i}{dx_i} = \frac{1}{J_i}\frac{\partial \phi}{\partial \xi_i}, \tag{23}$$

where J_i is the Jacobian of the transformation $x_i \to \xi_i$. Here, no summation over i is implied. Recalling that $[\mathsf{G}]_{\mathrm{ij}} = \partial u_{\mathrm{i}}/\partial x_{\mathrm{j}}$, the leading term of τ can be written more compactly as follows:

$$\tau = \frac{1}{12}\mathsf{G}_\xi \mathsf{G}_\xi^T + \mathcal{O}(\overline{\Delta}^4), \tag{24}$$

where the gradient in the mapped space $\boldsymbol{\xi}$ is represented by

$$\mathsf{G}_\xi = \mathsf{G}\mathsf{J}, \tag{25}$$

and J is the Jacobian of the transformation $\boldsymbol{x} \to \boldsymbol{\xi}$. Notice that this first term is generic for all practical filters[34] in the context of LES, i.e., filters with a Fourier transform starting with $\hat{G}(k) = 1 - k^2\overline{\Delta}/2 + \mathcal{O}(k^4)$. At the discrete level, for a Cartesian grid, the filter length in each direction is taken equal to the mesh size in the same direction, i.e., $\overline{\Delta}_i = \Delta x_i$. In this case, $\mathsf{J} = \Delta$ and $\mathsf{G}_\xi = \mathsf{G}_\Delta = \mathsf{G}\Delta$; therefore, the general expression given in Eq. (24) reduces to Eq. (16) for non-uniform Cartesian meshes and to the well-known gradient model[33] given in Eq. (15) for uniform grid spacings.

At this point, it becomes clear that the extension of the new subgrid characteristic length Δ_{lsq} [see Eq. (18) in Sec. III] for unstructured meshes relies on the computation of the Jacobian, J, on such grids. It is important to note that the gradient tensor, G, is actually being computed in any LES code. Below, the method to compute the Jacobian, J, is solely based on the discrete gradient operator; therefore, it can be easily applied to any existing code. Namely, using the matrix-vector notation, the discrete gradient operator is given by a block matrix

$$\boldsymbol{G}\boldsymbol{\phi}_h = \begin{pmatrix} \boldsymbol{G}_x \\ \boldsymbol{G}_y \\ \boldsymbol{G}_z \end{pmatrix} \boldsymbol{\phi}_h, \tag{26}$$

where $\boldsymbol{\phi}_h = (\phi_1, \phi_2, \ldots, \phi_n)^T \in \mathbb{R}^n$, n is the number of unknowns in our domain, and $\boldsymbol{G}_x$, $\boldsymbol{G}_y$, and $\boldsymbol{G}_z$ represent the discrete gradient operator for each spatial direction.

As a preview of things, we first consider the discretization of the gradient operator, $\boldsymbol{G}$, in one spatial direction with periodic boundary conditions. Let us consider three values of a smooth function $\phi(x)$: $\phi_{i-1} = \phi(x_{i-1})$, $\phi_i = \phi(x_i)$, and $\phi_{i+1} = \phi(x_{i+1})$ with $x_{i-1} = x_i - \Delta x$ and $x_{i+1} = x_i + \Delta x$. By a simple combination of Taylor series expansions of $\phi(x)$ around $x = x_i$, the well-known second-order accurate approximation of the derivative is as follows:

$$\frac{\partial \phi(x_i)}{\partial x} \approx \frac{\phi_{i+1} - \phi_{i-1}}{2\Delta x}. \tag{27}$$

Then with a uniformly meshed periodic direction, $\boldsymbol{G}_x$ results in a skew-symmetric circulant matrix of the form

$$\boldsymbol{G}_x = \frac{1}{2\Delta x}\mathrm{circ}(0, 1, 0, \cdots, 0, -1). \tag{28}$$

Thus, eigenvalues of $\boldsymbol{G}_x$ lie on the imaginary axis, $\lambda_k^{\boldsymbol{G}_x} \in \mathbb{I}$. Then, the eigenvalues can be easily bounded with the help of the Gershgorin circle theorem, i.e., $|\lambda_k^{\boldsymbol{G}_x}| \leq 1/\Delta x$. Notice that the upper bound exactly corresponds to the Jacobian, $J_x = 1/\Delta x$, of the mapping from the physical to the computational space for Cartesian grids. This idea can be extended to any grid or numerical method if we consider that, at the discrete level, the Jacobian, $\boldsymbol{J}$, is a diagonal matrix

$$\boldsymbol{J} \equiv \begin{pmatrix} \boldsymbol{J}_x & & \\ & \boldsymbol{J}_y & \\ & & \boldsymbol{J}_z \end{pmatrix}, \tag{29}$$

which, similar to the Cartesian case, guarantees that the spectral norm of the gradient in the so-called computational space $\boldsymbol{\mathcal{G}} \equiv \boldsymbol{J}\boldsymbol{G} = (\boldsymbol{\mathcal{G}}_x, \boldsymbol{\mathcal{G}}_y, \boldsymbol{\mathcal{G}}_z)^T$ is equal to or smaller than unity, i.e., $\|\boldsymbol{\mathcal{G}}\|_2 \leq 1$. This condition can easily be realized by using the Gershgorin circle theorem. Namely,

$$|\lambda_i^{\mathcal{G}_x} - \mathcal{G}_{ii}^x| \leq \sum_{j \neq i} |\mathcal{G}_{ij}^x| \quad \text{where} \quad \mathcal{G}_{ij}^x = \mathcal{J}_{ii}^x G_{ij}^x, \tag{30}$$

and $\mathcal{G}_{ij}^x = [\boldsymbol{\mathcal{G}}_x]_{i,j}$, $G_{ij}^x = [\boldsymbol{G}_x]_{i,j}$, and $\mathcal{J}_{ij}^x = [\boldsymbol{J}_x]_{i,j}$ are the coefficients of the matrices $\boldsymbol{\mathcal{G}}_x$, $\boldsymbol{G}_x$, and $\boldsymbol{J}_x$, respectively. Since $\boldsymbol{G}$ (also $\boldsymbol{\mathcal{G}}$) is usually a zero-diagonal matrix, i.e., $G_{ii} = 0$ (summation not implied), the condition $\|\boldsymbol{\mathcal{G}}\|_2 \leq 1$ simplifies to

$$|\lambda_i^{\mathcal{G}_x}| \leq \sum_{j \neq i} |\mathcal{G}_{ij}^x| \leq 1 \quad \forall i = 1, \ldots, n, \tag{31}$$

where n is the number of unknowns in our domain. Finally, recalling that the Jacobian must be positive, $\mathcal{J}_{ii} > 0$, and extending the previous analysis to the y and z directions, the following definitions for the Jacobian

$$\mathcal{J}_{ii}^x \equiv \frac{1}{\sum_{j \neq i} |G_{ij}^x|}, \quad \mathcal{J}_{ii}^y \equiv \frac{1}{\sum_{j \neq i} |G_{ij}^y|}, \quad \mathcal{J}_{ii}^z \equiv \frac{1}{\sum_{j \neq i} |G_{ij}^z|}, \tag{32}$$

guarantee that inequalities (31) are always satisfied. Here, no summation over i is implied. Therefore, the spectral norm of $\boldsymbol{G}_\xi$ is equal to or smaller than unity, i.e., $\|\boldsymbol{\mathcal{G}}\|_2 \leq 1$. In this way, the local Jacobian for the node i, J_i, is given by

$$\mathsf{J}_i = \begin{pmatrix} \mathcal{J}_{ii}^x & & \\ & \mathcal{J}_{ii}^y & \\ & & \mathcal{J}_{ii}^z \end{pmatrix}. \tag{33}$$

Notice that the definitions of the Jacobian given in Eq. (32) are solely based on the coefficients of the discrete gradient operator, $\boldsymbol{G}$. Therefore, there is no restriction regarding the type of grid and the numerical method. Moreover, it is worth noticing that for a Cartesian uniform mesh, this formula reduces to $\mathsf{J} = \mathrm{diag}(\Delta x, \Delta y, \Delta z)$ similar to the definition of Δ given in Eq. (13).

In this way, the subgrid characteristic length scale proposed in Sec. III is straightforwardly extended to unstructured meshes by simply replacing Δ in Eq. (18) by the local Jacobian, J_i, defined in Eqs. (32) and (33).

V. NUMERICAL RESULTS

A. Decaying homogeneous isotropic turbulence

The numerical simulation of decaying isotropic turbulence was chosen as a first case to test the novel definition of the subgrid characteristic length scale, Δ_{lsq}, proposed in Eq. (18). The configuration corresponds to the classical experiment of Comte-Bellot and Corrsin (CBC).[37] Large-eddy simulation results have been obtained using the Smagorinsky model for a set of (artificially) stretched meshes. Namely, results for pancake-like meshes with $32 \times 32 \times N_z$ and $N_z = \{32, 64, 128, 256, 512, 1024, 2048\}$ are displayed in Fig. 3 (top). As expected, for increasing values of N_z, the results obtained using the classical definition of Deardorff, given in Eq. (4), diverge. This is because the value of Δ_{vol} tends to zero for increasing N_z and, therefore, the subgrid-scale model switches off. This is not the case for the definition of Δ_{lsq} proposed in this work. Interestingly, the results rapidly converge for increasing values of N_z. Therefore, the proposed definition of the subgrid characteristic length, Δ_{lsq}, seems to minimize the effect of mesh anisotropies on the performance of subgrid-scale models.

Similar behavior is observed in Fig. 3 (bottom) for pencil-like meshes with $32 \times N_z \times N_z$ grid cells, where $N_z = \{32, 64, 128, 256, 512, 768\}$. In this case, the improper behavior of Deardorff's definition is even more evident because ν_e in Eq. (3) scales as $\mathcal{O}(\Delta z^{4/3})$ instead of the $\mathcal{O}(\Delta z^{2/3})$ scaling for the pancake-like meshes. Therefore, the model switches off even more rapidly. Furthermore, it is worth mentioning that in this case, this numerical artifact is visible for a wide range of wavenumbers, whereas for pancake-like meshes, only the smallest resolved scales are affected in a significant manner. On the other hand, LES results obtained with Δ_{lsq} also tend to converge for increasing values of N_z. Nevertheless, compared with the results obtained with pancake-like meshes, significant changes are observed for the first three meshes, i.e., $N_z = \{32, 64, 128\}$. This delay in the convergence of the LES results may be attributed to the fact that more scales are actually being solved in two spatial directions (instead of one for the pancake-like meshes). Therefore, the role of the LES model is lessened, and differences in the results can be probably attributed to the natural convergence for grid refinement. In any case, compared with the classical Deardorff approach, the newly proposed subgrid characteristic length scale strongly reduces the artificial effects caused by mesh anisotropies while providing a natural convergence.

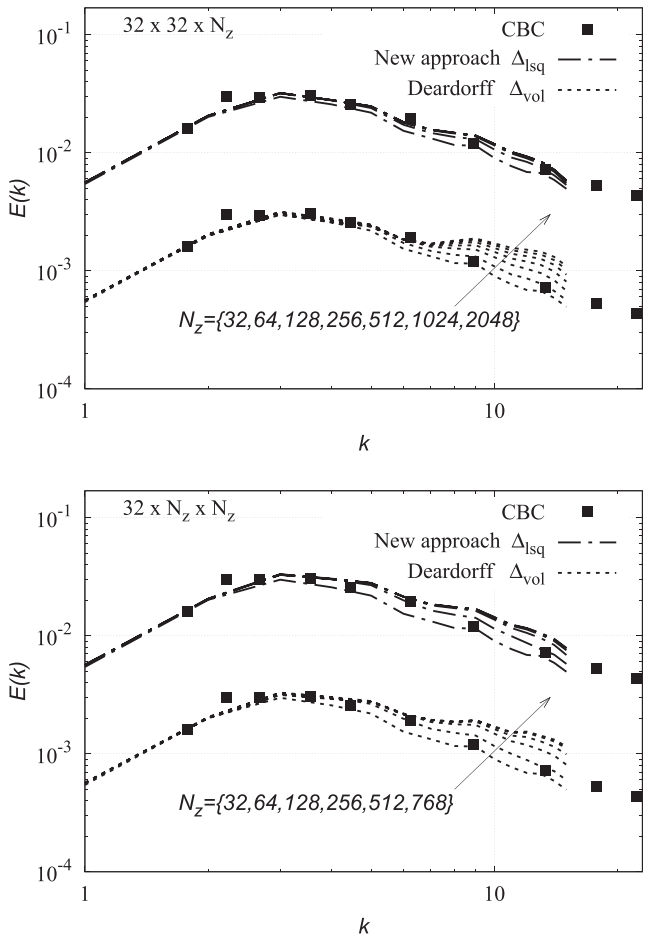

FIG. 3. Three-dimensional kinetic energy spectra as a function of computational wavenumber, for decaying isotropic turbulence corresponding to the experiment of Comte-Bellot and Corrsin.[37] LES results have been obtained using the Smagorinsky model for a set of anisotropic meshes with pancake-like (top) and pencil-like (bottom) control volumes. Results obtained with the novel definition of Δ_{lsq} proposed in Eq. (18) are compared with the classical definition proposed by Deardorff given in Eq. (4). For clarity, the latter results are shifted one decade down.

In order to analyze in more detail the effect of mesh anisotropies for different definitions of Δ, two physical quantities of interest have been studied: namely, the resolved kinetic energy and the resolved enstrophy. Results displayed in Fig. 4 have been obtained with the same pancake-like meshes (i.e., $32 \times 32 \times N_z$ grid cells, where $N_z = \{32, 64, 128, 256, 512, 1024, 2048\}$). In this case, apart from the new definition, Δ_{lsq}, and the Deardorff length scale, Δ_{vol}, two additional definitions have also been tested: the definition proposed by Scotti *et al.*,[25] Δ_{Sco}, given in Eq. (5) and the definition proposed by Mockett *et al.*,[31] $\tilde{\Delta}_{\omega}$, given in Eq. (10). It must be noted that for this comparison, we have chosen Δ_{Sco} because among all the definitions reviewed in Sec. I that solely depend on geometrical properties of the mesh (see property **P3** in Table I) this is the length scale that provides the best results. Regarding the flow-dependent definitions, we have chosen $\tilde{\Delta}_{\omega}$ because this definition was actually proposed as an improvement of the definition by Chauvet *et al.*[29] given in Eq. (9). The definition proposed by Shur *et al.*,[32] Δ_{SLA}, given in Eq. (11) has not been considered here because it is just a modification of $\tilde{\Delta}_{\omega}$ specifically adapted to trigger the Kelvin-Helmholtz instability in the initial part of shear layers.

As explained above, energy spectra obtained using Deardorff's length scale Δ_{vol} diverge for increasing values of N_z due to the fact that Δ_{vol} tends to zero and, therefore, the subgrid-scale model switches off. This effect becomes even more evident for the resolved enstrophy (see Fig. 4, bottom) since this lack of SGS dissipation mainly affects the smallest resolved scales. This physically improper behavior is strongly mitigated by other definitions of Δ. Namely, the definition proposed by Scotti *et al.*,[25] Δ_{Sco}, displays the weakest dependence with respect to N_z. As explained in Sec. I, this definition of Δ was proposed as a correction of the Deardorff definition, Δ_{vol}, for anisotropic meshes with the assumption of an isotropic turbulent regime. Therefore, it is not surprising that this definition behaves very robustly for a simulation of decaying homogeneous isotropic turbulence. On the other hand, we can observe that the novel definition, Δ_{lsq}, and the definition proposed by Mockett *et al.*,[31] $\tilde{\Delta}_{\omega}$, display a very similar behavior. Results for both resolved kinetic energy and enstrophy rapidly converge for increasing values of N_z. Even more interestingly, taking the CBC results as an indication

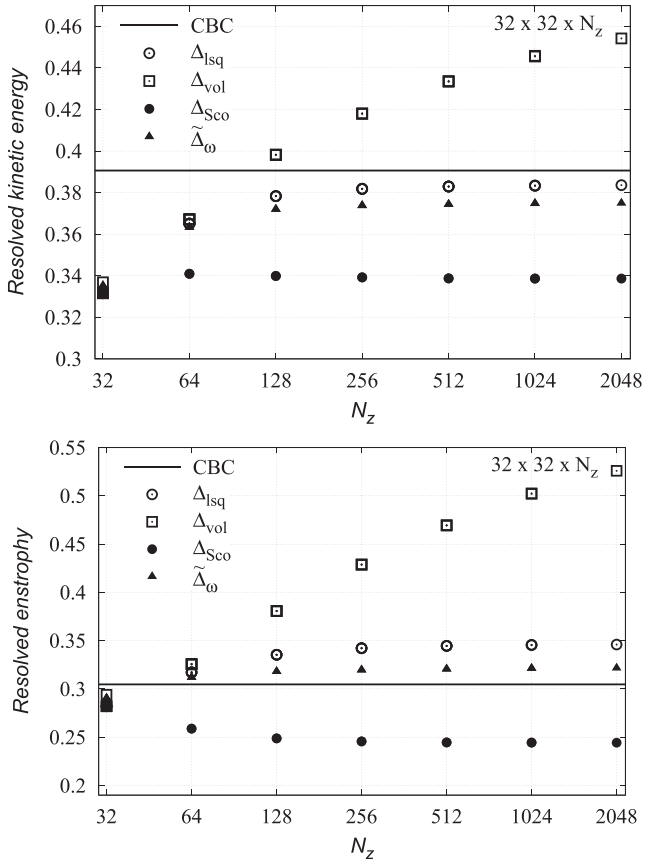

FIG. 4. Resolved kinetic energy (top) and enstrophy (bottom) as a function of the number of grid points, N_z, for decaying isotropic turbulence corresponding to the experiment of Comte-Bellot and Corrsin.[37] LES results have been obtained using the Smagorinsky model for a set of anisotropic meshes with pancake-like control volumes, i.e., $32 \times 32 \times N_z$. Results obtained with the novel definition of Δ_{lsq} proposed in Eq. (18) are compared with the definitions proposed by Deardorff,[22] Δ_{vol} [Eq. (4)], Scotti *et al.*,[25] Δ_{Sco} [Eq. (5)], and Mockett *et al.*,[31] $\tilde{\Delta}_{\omega}$ [Eq. (10)], respectively.

of the trend the data should have, both definitions lead to significantly better solutions compared with the original 32^3 mesh and the solution obtained with the definition proposed by Scotti *et al.*,[25] Δ_{Sco}.

B. Turbulent channel flow

To test the performance of the proposed definition of Δ_{lsq} with the presence of walls, simulations of a turbulent channel flow have also been considered. In this case, the code is based on a fourth-order symmetry-preserving finite-volume discretization[39] of the incompressible Navier-Stokes equations on structured staggered grids. Regarding the spatial discretization of the eddy-viscosity models, the approach proposed by Trias *et al.*[40] has been used in conjunction with the S3QR model recently proposed by Trias *et al.*[20] Namely,

$$\nu_e^{S3QR} = (C_{s3qr}\Delta)^2 Q_{\mathsf{GG}^T}^{-1} R_{\mathsf{GG}^T}^{5/6}, \tag{34}$$

where $C_{s3pq} = 0.762$, Q_{GG^T} and R_{GG^T} are the second and third invariants of the symmetric second-order tensor GG^T, and G is the gradient of the resolved velocity field, i.e., $\mathsf{G} \equiv \nabla\overline{\boldsymbol{u}}$. Similar to Vreman's model,[16] the S3QR model is also based on the invariants of the second-order tensor GG^T. However, it was designed to have the proper cubic near-wall behavior. Apart from this, it fulfills a set of desirable properties, namely, positiveness, locality, Galilean invariance, and it automatically switches off for laminar, 2D, and axisymmetric flows. Furthermore, it is well conditioned, has a low computational cost, and has no intrinsic limitations for statistically inhomogeneous flows.

Figure 5 shows the results obtained from numerical simulations of a turbulent channel flow at $Re_\tau = 395$ for a set of (artificially) refined grids. The results are compared with the DNS data of Moser *et al.*[38] The dimensions of the channel are taken equal to those of the DNS, i.e., $2\pi \times 2 \times \pi$. The starting point corresponds to a 32^3 mesh, which suffices to obtain good agreement with the DNS data. Therefore, the computational grid is very coarse in comparison with the DNS which was performed on a $256 \times 193 \times 192$ grid, i.e., the DNS used about 290 times more grid points than the first simulation. The grid points are uniformly distributed in the stream-wise and the span-wise directions, whereas the wall-normal points are distributed using hyperbolic sine functions. For the lower half of the channel, the distribution of points is given by

$$y_j = \sinh(\gamma j/N_y)/\sinh(\gamma/2) \quad j = 0, 1, \ldots, N_y/2, \tag{35}$$

where N_y denotes the number of grid points in the wall-normal direction. The stretching parameter, γ, is taken equal to 7. Then, the grid points in the upper half of the channel are computed by means of symmetry. With this distribution and $N_y = 32$, the first off-wall grid point is located at $y^+ \approx 2.6$, i.e., inside the viscous sublayer ($y^+ < 5$), whereas $\Delta x^+ \approx 77.5$ and $\Delta z^+ \approx 38.8$. Hence, the grid is highly anisotropic in the near-wall region, e.g., $\Delta x^+/\Delta y^+ \approx 14.7$ for the first off-wall control volume.

Apart from the first simulation, two additional meshes (with $N_z = 128$ and $N_z = 512$) have been used to investigate the effect of Δ. We chose to refine in the span-wise direction because simulation results should not be too much affected

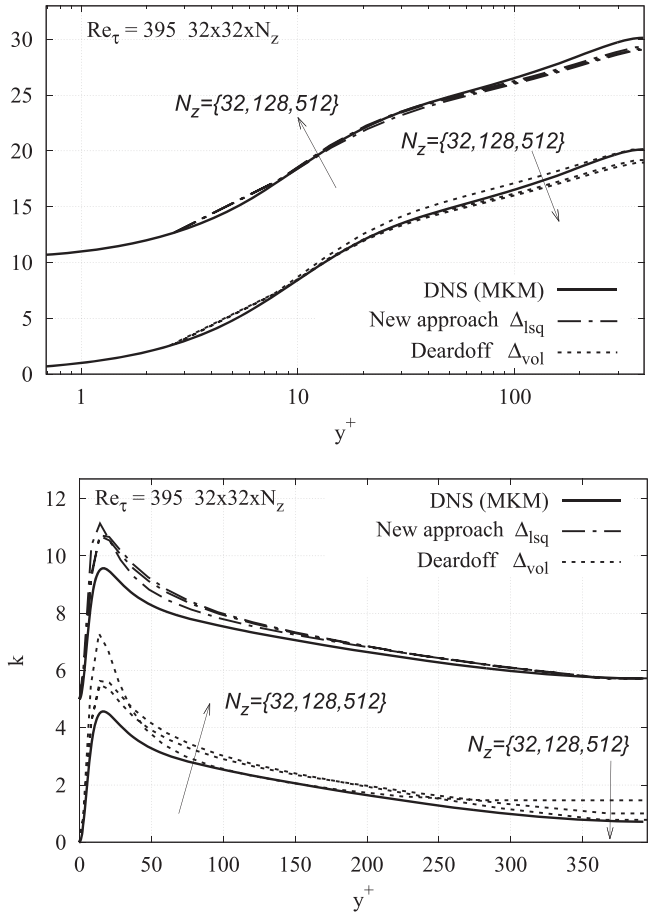

FIG. 5. Results for a turbulent channel flow at $Re_\tau = 395$ obtained with a set of anisotropic meshes using the S3PQ model.[20] Solid lines correspond to the direct numerical simulation of Moser *et al.*[38] Results obtained with the novel definition of Δ_{lsq} proposed in Eq. (18) are compared with the classical definition proposed by Deardorff given in Eq. (4). For clarity, the former results are shifted up. Top: mean streamwise velocity, $\langle u \rangle$. Bottom: turbulent kinetic energy, k.

compared with the other two directions. Again, as can be seen from Fig. 5, the results obtained with the new definition of Δ are much more robust to mesh anisotropies. It is remarkable that almost no changes are observed in the mean velocity profile when the newly proposed length scale is employed, whereas significant changes are observed for Deardorff's classical definition. Similar behavior is observed for the resolved turbulent kinetic energy, especially in the bulk region where results obtained with the new length scale are almost independent of the value of N_z.

To study the effect of mesh anisotropies for other definitions of Δ, results of the mean stream-wise velocity and turbulent kinetic energy at channel mid-height are displayed in Fig. 6. Similar to the previous test case, results obtained using the definitions proposed by Scotti *et al.*,[25] Δ_{Sco}, given in Eq. (5) and by Mockett *et al.*,[31] $\tilde{\Delta}_\omega$, given in Eq. (10) are also shown for comparison. In this case, similar to the simulation of decaying homogeneous isotropic turbulence, the results obtained using Deardorff's definition, Δ_{vol}, are strongly influenced by the mesh anisotropy. Again, other definitions tend to mitigate this. Despite the fact that it is based on the assumption of isotropic turbulence, the robustness of the definition

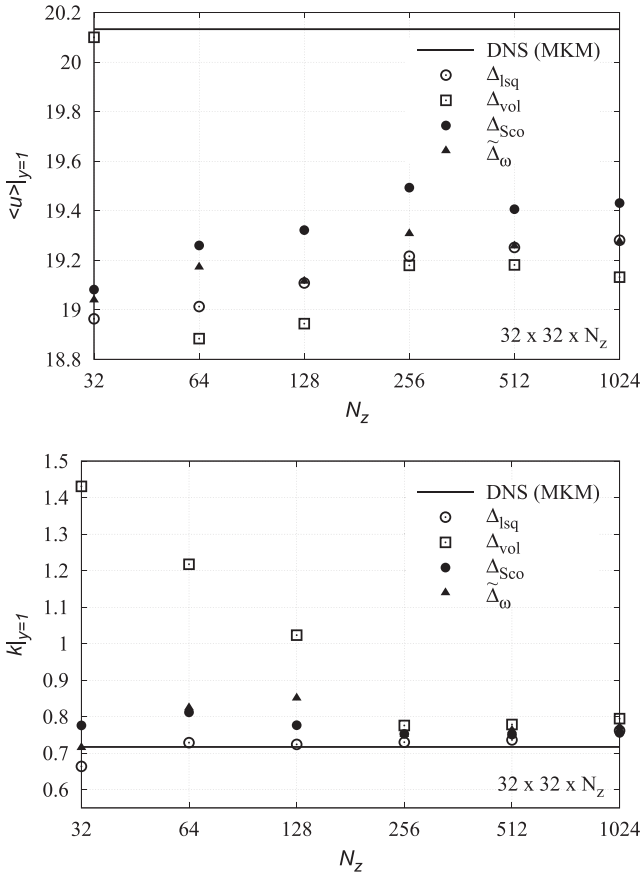

FIG. 6. Results for a turbulent channel flow at $Re_\tau = 395$ obtained with a set of anisotropic meshes using the S3PQ model.[20] Solid lines correspond to the direct numerical simulation of Moser *et al.*[38] Results obtained with the novel definition of Δ_{lsq} proposed in Eq. (18) are compared with the definitions proposed by Deardorff,[22] Δ_{vol} [Eq. (4)], Scotti *et al.*,[25] Δ_{Sco} [Eq. (5)], and Mockett *et al.*,[31] $\tilde{\Delta}_{\omega}$ [Eq. (10)], respectively. Top: mean streamwise velocity at channel mid-height, $\langle u \rangle|_{y=1}$. Bottom: turbulent kinetic energy at channel mid-height, $k|_{y=1}$.

proposed by Scotti *et al.*[25] regarding the turbulent kinetic energy is remarkable (see Fig. 6, bottom). However, its behavior is not so satisfactory regarding the average velocity field in the center of the channel (see Fig. 6, top). The least to be expected from numerical simulations of turbulence is a robust prediction of the mean flow; therefore, the new definition, Δ_{lsq}, and the definition $\tilde{\Delta}_{\omega}$ proposed by Mockett *et al.*[31] display a significantly more robust behavior in this regard. However, the definition $\tilde{\Delta}_{\omega}$ is not so robust when predicting the turbulent kinetic energy (see Fig. 6, bottom) where the results obtained with the new definition Δ_{lsq} are almost not affected when N_z increases. In summary, the results obtained using the new length scale, Δ_{lsq}, are at least as good as the best results obtained by other definitions with the advantage of having a much lower computational cost compared with $\tilde{\Delta}_{\omega}$ and being much easier to be used for unstructured grids.

C. Flow around a square cylinder

Finally, to test the performance of the proposed length scale with unstructured meshes, the turbulent flow around a square cylinder has been considered. In this case, the Reynolds number, $Re = UD/\nu = 22\,000$, is based on the inflow velocity, U, and the cylinder width, D. This is a challenging test case for LES. Apart from the well-known von Kármán vortex shedding in the wake region, this regime is characterized by the clear presence of Kelvin-Helmholtz vortical structures produced by the flow separation at the leading edge of the cylinder. The size of these vortices grows quickly, triggering turbulence before they reach the downstream corner of the cylinder. Actually, they break up into finer structures before being engulfed into the much larger von Kármán vortices. An additional motivation to choose this configuration is the fact that it has been studied before in many numerical and experimental studies. The reader is referred to our DNS study[41] and references therein for further details about the flow dynamics.

In the current work, we have carried out LESs on unstructured meshes using the NOISEtte code for the simulation of compressible turbulent flows in problems of aerodynamics and aeroacoustics. It is based on the family of high-accuracy finite-volume EBR (Edge-Based Reconstruction) schemes for unstructured meshes.[42] The EBR schemes provide at a low computing cost a higher accuracy than most Godunov-type second-order schemes on unstructured meshes. On translationally invariant (structured) meshes, the EBR schemes coincide with high-order (up to sixth-order) finite-difference schemes. Hybrid schemes with a combination of upwind and central-difference parts are used in LESs with automatic adaptation of the weights of the components in order to preserve numerical stability at a minimal numerical dissipation.

For the simulations, the 2D unstructured mesh displayed in Fig. 7 has been extruded in the span-wise direction. The

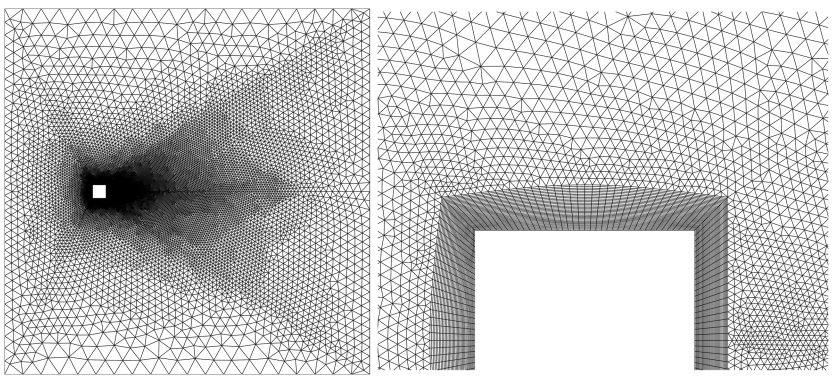

FIG. 7. Left: 2D section of the unstructured mesh used to perform the set of LESs of the turbulent flow around a square cylinder at $Re = 22\,000$. This (x, y)-section contains 19 524 nodes. Right: zoom around the obstacle.

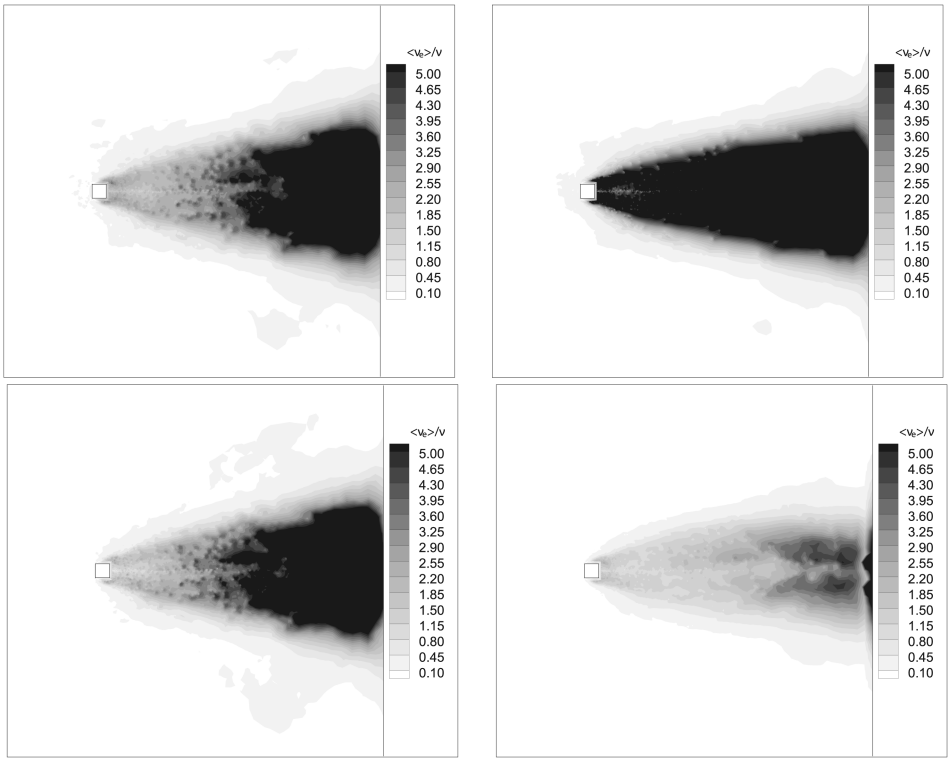

FIG. 8. Average eddy-viscosity, $\langle \nu_e \rangle$, divided by the kinematic viscosity, ν. Results for a turbulent flow around a square cylinder at $Re = 22\,000$ carried out using the S3PQ model[20] on a set of unstructured meshes obtained from the extrusion in the span-wise direction of the 2D mesh displayed in Fig. 7. Results obtained with the new definition, Δ_{lsq}, proposed in Eq. (18) (left) are compared with the classical definition proposed by Deardorff given in Eq. (4) (right). This is done for two meshes differing in the number of grid points in the span-wise direction: $N_z = 100$ (top) and $N_z = 1000$ (bottom).

resulting meshes have $19\,524 \times N_z$ control volumes, where N_z is the number of control volumes in the span-wise direction. In this study, we have considered three values for N_z, i.e., $N_z = \{50, 100, 1000\}$. The first two meshes are reasonable for an LES[43] whereas the mesh with $N_z = 1000$ is clearly too fine (even for a DNS[41]). The 2D base mesh (see Fig. 7, left) is basically composed of triangular elements, except for the region around the square cylinder where there are skewed quadrilateral elements (see Fig. 7, right). The dimensions of the computational domain are slightly smaller than in the DNS study:[41] $27D \times 27D \times 3D$ in the stream-wise, cross-stream, and span-wise directions, respectively. The upstream face of

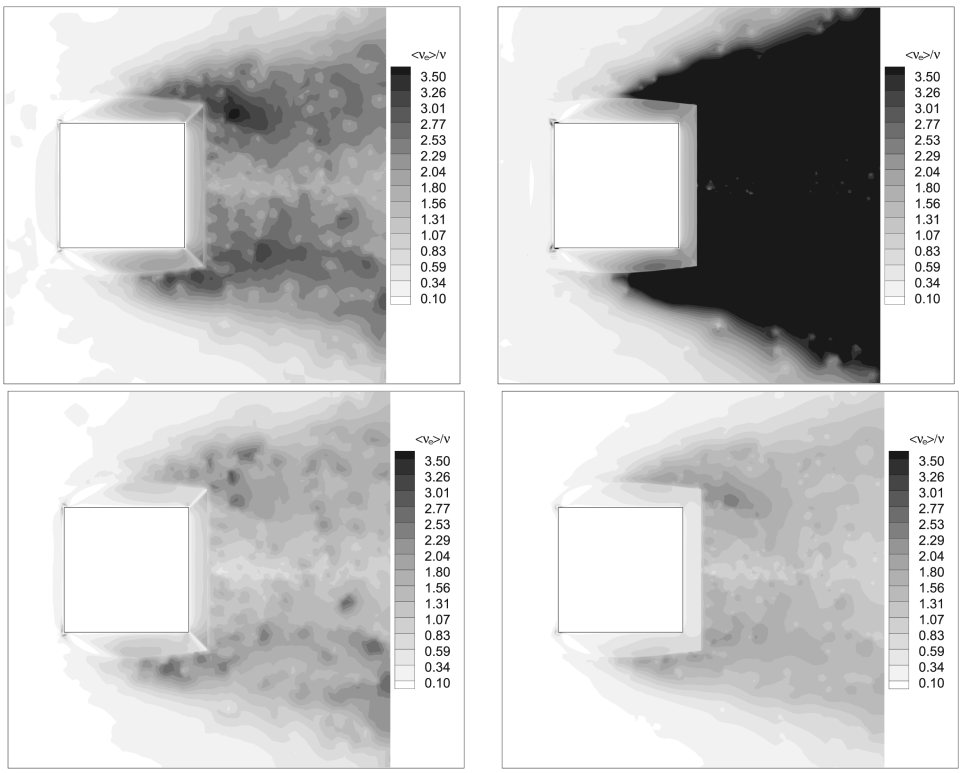

FIG. 9. The same as in Fig. 8. Zoom around the obstacle. Notice that the scale range has been properly modified.

the cylinder is located at $6.5D$ from the inflow and centered in the cross-stream direction. The origin of coordinates is placed at the center of the cylinder.

Similar to the turbulent channel flow, LES results have been obtained with the S3PQ model[20] using two definitions of Δ: the new definition, Δ_{lsq}, proposed in Eq. (18) and the classical definition proposed by Deardorff, given in Eq. (4). Results are compared with the experimental data of Lyn *et al.*[44] and our incompressible DNS results[41] which are taken as a reference. This DNS was carried out with a constant velocity profile, $\boldsymbol{u} = (U, 0, 0)$, at the inflow, convective boundary conditions, $\partial \boldsymbol{u}/\partial t + U \partial \boldsymbol{u}/\partial x = 0$, at the outflow, Neumann boundary condition in the cross-stream direction, $\partial \boldsymbol{u}/\partial y = 0$, periodic boundary conditions in the span-wise direction, and a no-slip condition at the surface of the cylinder. To make the comparison possible, present LESs are carried out with analogous boundary conditions and at a nearly incompressible Mach number ($M = 0.1$). Results are presented in dimensionless form where the reference length and velocity are the cylinder width, D, and the inflow velocity, U, respectively.

Results for the average eddy-viscosity, $\langle \nu_e \rangle$, divided by the kinematic viscosity, ν, are displayed in Figs. 8 and 9. Results for two meshes, i.e., $N_z = 100$ (top) and $N_z = 1000$ (bottom), are shown. As expected, values of ν_e obtained with Deardorff's length scale are strongly affected by such abnormal mesh anisotropies. In this regard, the ability of the new subgrid characteristic length, Δ_{lsq}, to adapt to these situations is remarkable. At first sight, the results displayed in Fig. 8 look almost identical for Δ_{lsq}, whereas very significant differences are observed for the Deardorff definition. A closer inspection (see Fig. 9) reveals how both definitions of Δ respond to the abrupt mesh transition between the near obstacle region and the rest of the domain (see Fig. 7, right). The new subgrid characteristic length tends to mitigate the effects of this mesh transition compared with the results obtained with the Deardorff definition. This difference becomes more evident for the mesh with $N_z = 1000$.

Sharp discontinuities in ν_e may have severe negative effects. Numerically, they can lead to more stringent time steps and potentially cause instabilities. The former increases the computational cost of the simulation, whereas the latter can be solved using a proper discretization of the viscous term.[40] From a physical point of view, this abnormal behavior of ν_e can negatively affect the quality of the results in an uncontrolled manner. In this regard, results of the average stream-wise velocity, $\langle u \rangle$, in the near cylinder region are displayed in Fig. 10. In this case, both the influence of the definition of Δ and the number of grid points in the span-wise direction, N_z, are rather small. This is a consequence of the fact that the turbulence model itself has a relatively low impact in the near-wall region, especially near the upstream corner. Therefore, discrepancies with the DNS results in this region can simply be attributed to insufficient grid resolution. This region is actually characterized by the formation of small vortices in the shear layer due to the Kelvin-Helmholtz instability that are rapidly convected downstream. The size of these vortices grows quickly, triggering turbulence before they reach the downstream corner of the cylinder. Interestingly, much better agreement with the DNS results

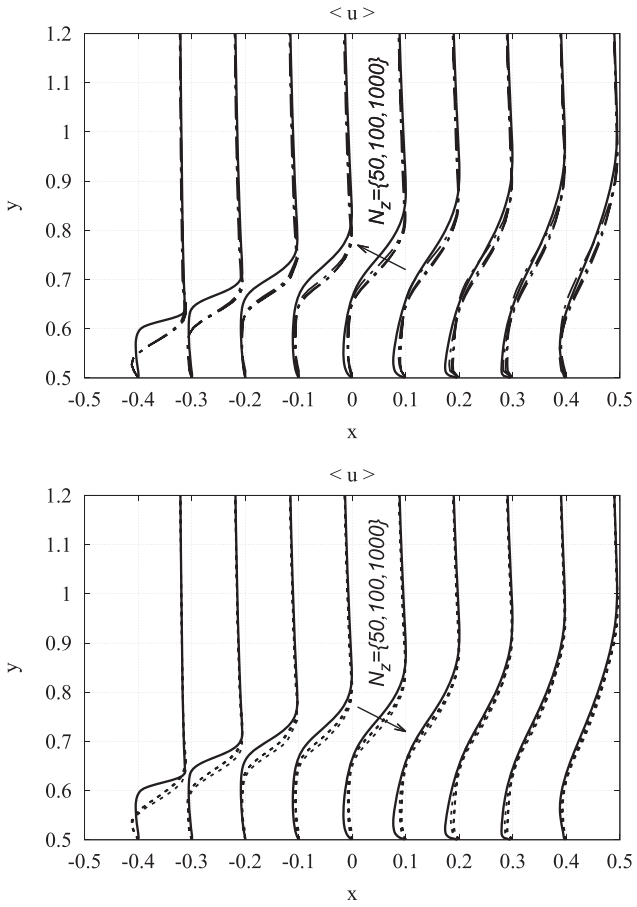

FIG. 10. Profiles of the average stream-wise velocity, $\langle u \rangle$, in the near-wall region. Results correspond to a turbulent flow around a square cylinder at $Re = 22\,000$ carried out using the S3PQ model[20] on a set of unstructured meshes obtained from the extrusion in the span-wise direction, i.e., $N_z = \{50, 100, 1000\}$, of the 2D mesh displayed in Fig. 7. Solid lines correspond to the DNS results of Trias *et al.*[41] Results obtained with the novel definition Δ_{lsq} (top) proposed in Eq. (18) are compared with the classical definition proposed by Deardorff (bottom) given in Eq. (4).

is achieved in this region. Apart from this, it is also interesting to observe that results obtained with the new subgrid characteristic length, Δ_{lsq}, become closer to the DNS results when N_z increases. The results obtained with the Deardorff definition display an opposite behavior. These trends remain the same in the wake region where differences between both approaches are more visible. This is clearly observed in the average stream-wise velocity profiles displayed in Fig. 11. The anomalous behavior of the Deardorff definition when refining in the span-wise direction becomes more evident further downstream. The most relevant results in this regard are the average stream-wise velocity profiles in the domain centerline displayed in Fig. 12. Results obtained with $N_z = 1000$ and the Deardorff definition of Δ are completely different from those obtained with $N_z = 50$ and $N_z = 100$, showing that the definition of Δ itself can have a very negative impact on the performance of an SGS model. Such an abnormal behavior is not observed with the new subgrid characteristic length, Δ_{lsq}.

These results confirm the findings of the first two test cases (i.e., decaying isotropic turbulence and a turbulent channel flow): compared with the Deardorff definition, Δ_{vol}, the

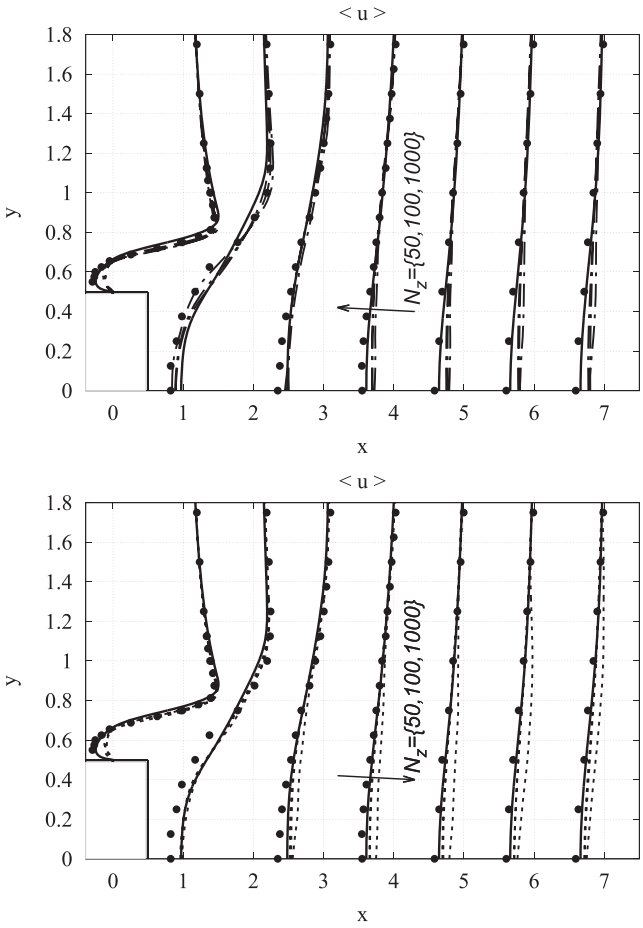

FIG. 11. The same as in Fig. 10. In this case, profiles are in the wake region. Experimental results of Lyn *et al.*[44] (solid circles) are also displayed for comparison.

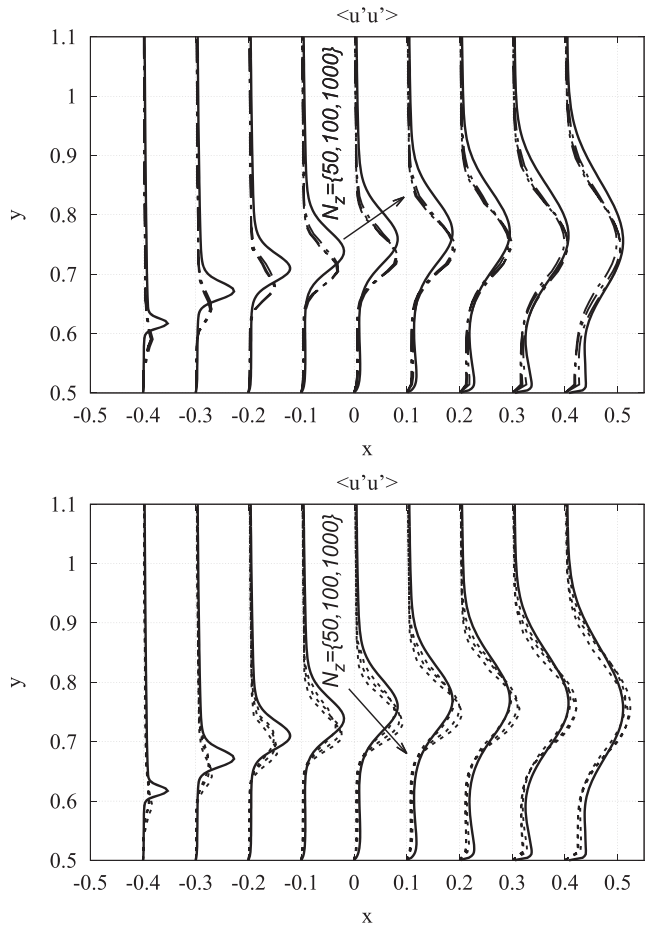

FIG. 13. Profiles of the stream-wise Reynolds stresses, $\langle u'u' \rangle$, in the near-wall region. Results correspond to a turbulent flow around a square cylinder at Re = 22 000 carried out using the S3PQ model[20] on a set of unstructured meshes obtained from the extrusion in the span-wise direction, i.e., $N_z = \{50, 100, 1000\}$, of the 2D mesh displayed in Fig. 7. Solid lines correspond to the DNS results of Trias *et al.*[41] Results obtained with the novel definition Δ_{lsq} (top) proposed in Eq. (18) are compared with the classical definition proposed by Deardorff (bottom) given in Eq. (4).

proposed definition, Δ_{lsq}, is much more robust with respect to mesh anisotropies. For those two cases, it was also seen that results using Δ_{lsq} are at least as good as the best results obtained with other definitions. Furthermore, it was also observed that these trends are even more evident for turbulent statistics. Here, the results for the stream-wise Reynolds stresses, $\langle u'u' \rangle$, in the near-wall region displayed in Fig. 13 seem to confirm this. The robustness of the new definition, Δ_{lsq}, in the shear layer region where there is almost a perfect match for the three meshes is remarkable (N_z = {50, 100, 1000}), while differences are observed for the classical Deardorff definition, Δ_{vol}. The new definition, Δ_{lsq}, is even more robust if we consider that in this shear layer region, there is an abrupt mesh transition from structured hexahedral elements to unstructured triangular prism (see Fig. 7, right).

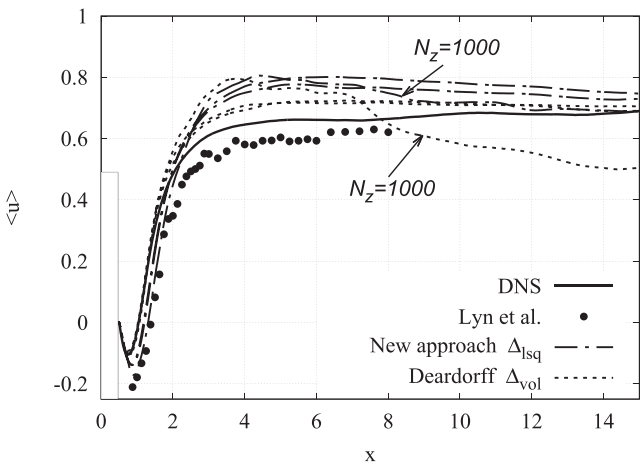

FIG. 12. The same as in Fig. 10. In this case, average stream-wise velocity profiles are in the domain centerline. Experimental results of Lyn *et al.*[44] are also displayed for comparison.

VI. CONCLUDING REMARKS

In this work, a novel definition of the subgrid characteristic length, Δ, has been proposed with the aim to answer the following research question: *Can we find a simple and robust definition of* Δ *that minimizes the effect of mesh anisotropies on the performance of SGS models*? In this respect, due to its simplicity and mathematical properties, we consider the flow-dependent Δ_{lsq} given in Eq. (18) a very good candidate. Namely, it is locally defined, frame invariant, well bounded (see properties **P1** and **P2** in Sec. II), and well conditioned,

and it has a low computational cost (property **P5**). Moreover, a simple extension of this length scale for unstructured grids (property **P4**) has been proposed in Sec. IV: it basically consists in replacing Δ in Eq. (18) by the local Jacobian, J_i, defined in Eqs. (33) and (32). Finally, from the definition of Δ_{lsq}, it is obvious that it is dependent on the local flow topology given by the gradient of the resolved velocity, $\mathsf{G} \equiv \nabla\overline{\boldsymbol{u}}$ (property **P3**). In this respect, analytical analysis for simple flow configurations points out the adequacy of the proposed definition. Numerically, it has been successfully tested for simulations of decaying homogeneous isotropic turbulence and a turbulent channel flow at $Re_\tau = 395$ using (artificially) refined grids. Comparisons with the classical length scale of Deardorff have shown that the proposed definition is much more robust with respect to mesh anisotropies. Due to these findings and its simplicity, we think the currently proposed length scale has a great potential to be used in subgrid-scale models in complex geometries where highly skewed (unstructured) meshes are present.

ACKNOWLEDGMENTS

This work has been financially supported by the *Ministerio de Economía y Competitividad*, Spain (No. ENE2014-60577-R). F.X.T. is supported by a *Ramón y Cajal* postdoctoral Contract (No. RYC-2012-11996) financed by the *Ministerio de Economía y Competitividad*, Spain. A.G. is supported by the Russian Science Foundation (Project No. 15-11-30039). M.H.S. is supported by the Free Competition in the Physical Sciences (Project No. 613.001.212), which is financed by the Netherlands Organization for Scientific Research (NWO). Part of this research was conducted at the CTR Summer Program 2016: F.X.T., M.H.S., and R.W.C.P.V. thank the Center for Turbulence Research (CTR) at Stanford University for hospitality and financial support. This work has been carried out using computing resources of the Barcelona Supercomputing Center and the Federal collective usage center "Complex for Simulation and Data Processing for Mega-science Facilities" at NRC "Kurchatov Institute", http://ckp.nrcki.ru/.

[1]D. K. Lilly, "The representation of small scale turbulence in numerical simulation experiments," in *IBM Scientific Computing Symposium on Environmental Sciences*, edited by H. H. Goldstine (IBM, Yorktown Heights, NY, 1967), pp. 195–210.
[2]J. Smagorinsky, "General circulation experiments with the primitive equations," Mon. Weather Rev. **91**, 99–164 (1963).
[3]D. A. Donzis and K. R. Sreenivasan, "The bottleneck effect and the Kolmogorov constant in isotropic turbulence," J. Fluid Mech. **657**, 171–188 (2010).
[4]P. Moin and J. Kim, "Numerical investigations of turbulent channel flow," J. Fluid Mech. **118**, 341–377 (1982).
[5]U. Piomelli, J. Ferziger, P. Moin, and J. Kim, "New approximate boundary conditions for large eddy simulations of wall-bounded flows," Phys. Fluids A **1**, 1061–1068 (1989).
[6]M. Germano, U. Piomelli, P. Moin, and W. H. Cabot, "A dynamic subgrid-scale eddy viscosity model," Phys. Fluids A **3**, 1760–1765 (1991).
[7]D. K. Lilly, "A proposed modification of the Germano subgrid-scale closure method," Phys. Fluids A **4**, 633–635 (1992).
[8]S. Ghosal, T. S. Lund, P. Moin, and K. Akselvoll, "A dynamic localization model for large-eddy simulation of turbulent flows," J. Fluid Mech. **286**, 229–255 (1995).
[9]C. Meneveau, T. S. Lund, and W. H. Cabot, "A Lagrangian dynamic subgrid-scale model of turbulence," J. Fluid Mech. **319**, 353–385 (1996).
[10]N. Park, S. Lee, J. Lee, and H. Choi, "A dynamic subgrid-scale eddy viscosity model with a global model coefficient," Phys. Fluids **18**(12), 125109 (2006).
[11]M. Germano, "Turbulence: The filtering approach," J. Fluid Mech. **238**, 325–336 (1992).
[12]D. You and P. Moin, "A dynamic global-coefficient subgrid-scale eddy-viscosity model for large-eddy simulation in complex geometries," Phys. Fluids **19**(6), 065110 (2007).
[13]A. E. Tejada-Martínez and K. E. Jansen, "A dynamic Smagorinsky model with dynamic determination of the filter width ratio," Phys. Fluids **16**(7), 2514–2528 (2004).
[14]A. E. Tejada-Martínez and K. E. Jansen, "A parameter-free dynamic subgrid-scale model for large-eddy simulation," Comput. Methods Appl. Mech. Eng. **195**, 2919–2938 (2006).
[15]F. Nicoud and F. Ducros, "Subgrid-scale stress modelling based on the square of the velocity gradient tensor," Flow, Turbul. Combust. **62**(3), 183–200 (1999).
[16]A. W. Vreman, "An eddy-viscosity subgrid-scale model for turbulent shear flow: Algebraic theory and applications," Phys. Fluids **16**(10), 3670–3681 (2004).
[17]R. Verstappen, "When does eddy viscosity damp subfilter scales sufficiently?," J. Sci. Comput. **49**(1), 94–110 (2011).
[18]F. Nicoud, H. B. Toda, O. Cabrit, S. Bose, and J. Lee, "Using singular values to build a subgrid-scale model for large eddy simulations," Phys. Fluids **23**(8), 085106 (2011).
[19]S. Ryu and G. Iaccarino, "A subgrid-scale eddy-viscosity model based on the volumetric strain-stretching," Phys. Fluids **26**(6), 065107 (2014).
[20]F. X. Trias, D. Folch, A. Gorobets, and A. Oliva, "Building proper invariants for eddy-viscosity subgrid-scale models," Phys. Fluids **27**(6), 065103 (2015).
[21]M. H. Silvis, R. A. Remmerswaal, and R. Verstappen, "Physical consistency of subgrid-scale models for large-eddy simulation of incompressible turbulent flows," Phys. Fluids **29**(1), 015105 (2017).
[22]J. W. Deardorff, "Numerical study of three-dimensional turbulent channel flow at large Reynolds numbers," J. Fluid Mech. **41**, 453–480 (1970).
[23]U. Schumann, "Subgrid scale model for finite difference simulations of turbulent flows in plane channels and annuli," J. Comput. Phys. **18**, 376–404 (1975).
[24]D. K. Lilly, "The length scale for sub-grid-scale parametrization with anisotropic resolution," Center for Turbulence Research, Annual Research Briefs, 1998.
[25]A. Scotti, C. Meneveau, and D. K. Lilly, "Generalized Smagorinsky model for anisotropic grids," Phys. Fluids A **5**(9), 2306–2308 (1993).
[26]A. Scotti, C. Meneveau, and M. Fatica, "Dynamics Smagorinsky model on anisotropic grids," Phys. Fluids **9**(6), 1856–1858 (1997).
[27]C. E. Colosqui and A. A. Oberai, "Generalized Smagorinsky model in physical space," Comput. Fluids **37**, 207–217 (2008).
[28]P. R. Spalart, W. H. Jou, M. Strelets, and S. R. Allmaras, "Comments on the feasibility of LES for wings, and on a hybrid RANS/LES approach," in *Advances in DES/LES*, edited by C. Liu and Z. Liu (Greyden Press, Columbus, OH, 1997).
[29]N. Chauvet, S. Deck, and L. Jacquin, "Zonal detached eddy simulation of a controlled propulsive jet," AIAA J. **45**(10), 2458–2473 (2007).
[30]S. Deck, "Recent improvements in the zonal detached eddy simulation (ZDES) formulation," Theor. Comput. Fluid Dyn. **26**(6), 523–550 (2012).
[31]C. Mockett, M. Fuchs, A. Garbaruk, M. Shur, P. Spalart, M. Strelets, F. Thiele, and A. Travin, "Two non-zonal approaches to accelerate RANS to LES transition of free shear layers in DES," in *Progress in Hybrid RANS-LES Modelling*, Notes on Numerical Fluid Mechanics and Multidisciplinary Design Vol. 130, edited by S. Girimaji, W. Haase, S.-H. Peng, and D. Schwamborn (Springer International Publishing, 2015), pp. 187–201.
[32]M. L. Shur, P. R. Spalart, M. K. Strelets, and A. K. Travin, "An enhanced version of DES with rapid transition from RANS to LES in separated flows," Flow, Turbul. Combust. **95**, 709–737 (2015).
[33]R. A. Clark, J. H. Ferziger, and W. C. Reynolds, "Evaluation of subgrid-scale models using an accurately simulated turbulent flow," J. Fluid Mech. **91**, 1–16 (1979).
[34]G. S. Winckelmans, A. A. Wray, O. V. Vasilyev, and H. Jeanmart, "Explicit-filtering large-eddy simulation using tensor-diffusivity model supplemented by a dynamic Smagorinsky term," Phys. Fluids **13**(5), 1385–1403 (2001).
[35]M. H. Silvis, F. X. Trias, M. Abkar, H. J. Bae, A. Lozano-Durán, and R. W. C. P. Verstappen, "Exploring nonlinear subgrid-scale models and

new characteristic length scales for large-eddy simulation," in Proceedings of the Summer Program 2016, Center for Turbulence Research, Stanford University, 2016.
[36]F. X. Trias, A. Gorobets, A. P. Duben, and A. Oliva, "Building a new subgrid characteristic length for LES," in Fourth International Workshop Computational Experiment in Aeroacoustics, Svetlogorsk, Russia, September 2016.
[37]G. Comte-Bellot and S. Corrsin, "Simple Eulerian time correlation of full- and narrow-band velocity signals in grid-generated, isotropic turbulence," J. Fluid Mech. **48**, 273–337 (1971).
[38]R. D. Moser, J. Kim, and N. N. Mansour, "Direct numerical simulation of turbulent channel flow up to $Re_\tau = 590$," Phys. Fluids **11**, 943–945 (1999).
[39]R. W. C. P. Verstappen and A. E. P. Veldman, "Symmetry-preserving discretization of turbulent flow," J. Comput. Phys. **187**, 343–368 (2003).
[40]F. X. Trias, A. Gorobets, and A. Oliva, "A simple approach to discretize the viscous term with spatially varying (eddy-)viscosity," J. Comput. Phys. **253**, 405–417 (2013).
[41]F. X. Trias, A. Gorobets, and A. Oliva, "Turbulent flow around a square cylinder at Reynolds number 22000: A DNS study," Comput. Fluids **123**, 87–98 (2015).
[42]I. Abalakin, P. Bakhvalov, and T. Kozubskaya, "Edge-based reconstruction schemes for unstructured tetrahedral meshes," Int. J. Numer. Methods Fluids **81**(6), 331–356 (2016).
[43]M. Minguez, C. Brun, R. Pasquetti, and E. Serre, "Experimental and high-order LES analysis of the flow in near-wall region of a square cylinder," Int. J. Heat Fluid Flow **32**(3), 558–566 (2011).
[44]D. Lyn, S. Einav, W. Rodi, and J. Park, "A laser Doppler velocimetry study of ensemble-averaged characteristics of the turbulent near wake of a square cylinder," J. Fluid Mech. **304**, 285–319 (1995).